THRESHOLD FOR TWO-STREAM INSTABILITIES

M. V. NEZLIN, M. I. TAKTAKISHVILI and A. S. TRUBNIKOV

Submitted February 8, 1968

Zh. Eksp. Teor. Fiz. 55, 397–414 (August, 1968)

An experimental investigation has been made of the threshold (critical current) for the excitation of the electron-ion two-stream instability and the drift-two-stream instability; the spatial structure and the dispersion properties of the electron-ion oscillations have also been studied. The results that are obtained verify the linear theory that describes the instability of a charged-particle beam in a plasma. Both of these instabilities play a role in the anomalous diffusion of plasma across a magnetic field and in the acceleration of plasma ions to energies comparable with the energies of the electrons in the beam. One of the instabilities (the drift-two-stream instability) is the cause for the limitation (cutoff) of the current in a quasi-neutral electron beam.

INTRODUCTION AND SUMMARY OF THEORETICAL RESULTS

IT is the purpose of the present paper to present an experimental verification of the linear theory of the instability of a monoenergetic beam of charged particles in a plasma. The method is based on the measurement of the instability threshold.

The existence of a threshold for the two-stream instability follows directly from the linear theory. For example, in the one-dimensional case the instability arises under the following conditions [cf. Eq. (7) and footnote 1]

$$(\omega_1^2)^{1/3} + (\omega_2^2)^{1/3} \gg (k^2u^2)^{1/3}, \tag{1}$$

where $\omega_1 = (4\pi n_1 e^2/m_1)^{1/2}$ and $\omega_2 = (4\pi n_2 e^2/m_2)^{1/2}$ are the plasma frequencies for the beam and the plasma; n_1 and n_2 and m_1 and m_2 are the densities and masses for the particles; u is the velocity of the beam particles; $k = 2\pi/\lambda$ is the wave number; λ is the wavelength of the oscillations (longitudinal) that are excited. It is evident that when

$$\omega_2^2 < k^2u^2 \tag{2}$$

the instability can occur only if the density of the beam exceeds some critical threshold value; if (2) is not satisfied then that threshold is not reached.

Below, in order to be definite, we shall assume that the particles in the beam are electrons. In this case the instabilities will be called either the electron-electron instability or the electron-ion instability, depending on which particles in the plasma (electrons or ions) play the basic role in the excitation of the oscillations.

The threshold for the electron-electron two-stream instability has been measured in[1], in which good agreement is reported with the existing theory. In the present work we describe the results of measurements of the thresholds for the electron-ion instabilities. These measurements have been carried out for a two-component system of charged particles consisting of the electrons in the beam and the positive ions, which neutralize the space charge of the electrons; the density of electrons in the plasma is negligibly small compared with the density of the beam. This system has been chosen for the measurements in order to make it possible to distinguish electron-ion oscillations from electron-electron oscillations.

A theoretical analysis of the threshold for the electron-ion stability has been given by Budker[2] and later by Buneman.[3] In the present work, however, we shall use the more useful derivation of the expression for the threshold given by Vedenov, Velikhov and Sagdeev.[4] Having in mind the comparison of theory with experiment, we treat a monoenergetic quasi-neutral electron beam in a longitudinal magnetic field whose magnitude H is such as to satisfy the conditions

$$\begin{aligned} \omega_{He} &\gg \omega_1, \\ \omega_{Hi} &\ll \omega \ll \omega_{He}, \end{aligned} \tag{3}$$

where $\omega_{Hi} = eH/Mc$ and $\omega_{He} = eH/mc$ are the gyrofrequencies for the ions and the electrons, ω_1 is the plasma frequency for the beam electrons and ω is the frequency of the electron-ion oscillations that are being analyzed. The conditions in (3) means that the electrons are "magnetized" and can only oscillate along **H** (if the electric field associated with the oscillations exhibits axial symmetry), while the ions are not magnetized and oscillate along the electric field (in particular, they can move freely in the direction perpendicular to **H**). We shall assume that the oscillations are axially symmetric. The dispersion relation for these waves is of the form

$$\frac{\omega_1^2 k_z^2/k^2}{(\omega - k_z u)^2} + \frac{\omega_+^2}{\omega^2} = 1, \tag{4}$$

where ω_+ is the ion-plasma frequency, k is the total wave number: $k^2 = k_z^2 + k_r^2$, $k_z = 2\pi/\lambda_z$ is the longitudinal wave number and k_r is the radial wave number, given by the relations[5]

$$k_r^2 \approx \begin{cases} \dfrac{1}{a^2 \ln \sqrt{R_0/a}} & \text{when } \lambda_z > 2\pi R_0 \\ \dfrac{1}{a^2 \ln \sqrt{\lambda_z/2\pi a}} & \text{when } \lambda_z < 2\pi R_0, \end{cases} \tag{5}$$

where R_0 is the radius of the equipotential cylinder along the axis of which the beam propagates.

We shall assume that standing waves are set up along the beam so that the wave number is specified (for example $k_z = n\pi/L$, $n = 1, 2, 3, \ldots$ where L is

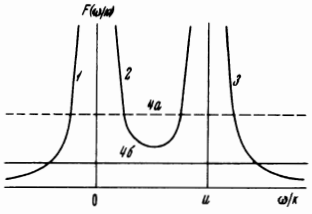

FIG. 1. Dispersion curves. 1, 2, 3) branches of the function $F(\omega, k)$ for k = const, the line 4) $F(\omega, k) \equiv 1$, a) stability, b) instability.

the length of the beam); we then solve the dispersion relation (4) with respect to ω taking k_z = const.

Denoting the left side of Eq. (4) by $F(\omega)$ we can now plot the branches of the function $F(\omega)$ (cf. Fig. 1). It is evident that the instability arises when the center branch of the function $F(\omega)$, shown as the curve marked 2, no longer intersects the horizontal line $F(\omega) = 1$. In this case the number of points of intersection of the branches 1–3 with the line 4 (two) will be smaller than the number of roots of Eq. (4) (four) and the missing two roots of ω are complex (complex conjugate), one of these corresponding to the excitation of oscillations. In the critical regime (branch 2 tangent to curve 4) $\partial F(\omega)/\partial\omega = 0$ and the oscillations frequency is given by

$$\omega_k = k_z u \Big/ \left[1 + \left(\frac{M}{m}\frac{k_z^2}{k^2}\right)^{1/3}\right]. \tag{6}$$

Substituting ω_k from Eq. (6) in Eq. (4) we can find the threshold (critical) density n_{1k} and the threshold current I_k for the beam:

$$I_k \equiv \pi a^2 n_{1k} e u \equiv \frac{ma^2}{4e}\omega_{1k}{}^2 u = \frac{ma^2}{4e}k^2 u^3 \Big/ \left[1 + \left(\frac{m}{M}\frac{k^2}{k_z^2}\right)^{1/3}\right]^3, \tag{7}$$

where ω_{1k} is the plasma frequency of the beam at the critical (threshold) point and a is the radius of the beam.[1)]

In the further analysis it will be important to estimate the magnitude of the second term in the rectangular brackets in the denominator of Eq. (7). For the typical conditions reported here we have $M/m = 5.6 \times 10^4$ (nitrogen) $k_z = 2\pi/\lambda_z = \pi/L$, $L \approx 10^2$ cm (L is the length of the beam), $a \approx 0.5$ cm, $R_0 = 15$ cm, $k^2 \approx 2.4$ cm^{-2}. Under these conditions

$$\left(\frac{m}{M}\frac{k^2}{k_z^2}\right)^{1/3} \approx 0.4, \qquad \omega_k \approx \frac{k_z u}{4}, \qquad \omega_{1k}{}^2 \approx \frac{k^2 u^2}{2.5}. \tag{8}$$

Taking account of Eq. (8) and using Eq. (6) we see that the excitation mechanism being considered here is not the Cerenkov mechanism (the phase velocity of the waves ω/k_z is much smaller than the velocity of the electrons in the beam); the mechanism is actually the anomalous Doppler effect.[6]

Following the work of Budker and Buneman[2,3] the theory of electron-ion oscillations took a substantial step forward in the work of Mikhaĭlovskiĭ[7] and Rukhadze and his collaborators[8] (cf. also Vladimirov[9]). These authors considered the drift instability of an electron beam in a plasma. We will call this the drift-two-stream instability. The difference between this instability and the usual two-stream instability[2,3] is the following. In the ordinary two-stream instability the waves that are excited exhibit axial symmetry: the electric field of the waves has only two components, a longitudinal component E_z and a radial component E_r. However, in the drift-two-stream instability the axial symmetry of the waves is disturbed: there is in addition a third (azimuthal) component of the electric field in the wave E_φ, the appearance of which is related to the spatial (radial) inhomogeneity of the beam. Correspondingly, the wave vector k consists of three components: $k^2 = k_z^2 + k_r^2 + k_\varphi^2$ where $k_\varphi = s/a$ is the azimuthal wave number, s is the azimuthal mode number (the number of wavelengths around the beam perimeter) and a is the characteristic dimension of the radial inhomogeneity of the density in the beam. This modification of the spatial structure of the wave introduces an important modification in the threshold for the instability. The point here is that the threshold for excitation of electron-ion waves that are not axially symmetric is given by[10]

$$I_k \approx \frac{ma^2}{4e}\frac{k^2 u^3}{[1 + 2k_\varphi u/a\omega_{He}k_z]}. \tag{9}$$

It will be evident that with relatively modest magnetic fields, in which case the second term in the denominator in Eq. (9) is large compared with unity, the threshold in (9) is significantly smaller than the threshold given in (7).[2)]

The results of the theory are illustrated in the table. In order to make a more complete comparison of theory with experiment, in addition to showing electron-ion instabilities we have also included two electron-electron instabilities. One of these (the fourth row) arises if the density of the electrons in the plasma n_2 is not negligibly small compared with the beam density, for example $n_2 \gtrsim n_1$. The second (Pierce) instability arises as a result of the interaction of electrons in the beam with the electrons in external circuit structures which maintain equipotentials in the volume within which the beam propagates.[11,12]

An examination of the table leads to the following conclusions. Whereas the thresholds for the three usual two-stream instabilities do not depend on H [for the condition in Eq. (3)] and depend uniquely on u, ($I_k \sim u^3$), the threshold for the drift-two-stream instability is very sensitive to H and is a more complicated function of u. For example, at relatively weak magnetic fields, in which case

$$2k_\varphi u / a\omega_{He}k_z \gg 1, \tag{10}$$

the threshold is proportional to Hu^2; for the condition that is the inverse of (10) the threshold is independent of H and is proportional to u^3. It also follows from the table that with a gradual increase in beam current the sequence of excitation for various instabilities will depend on the system parameters, in particular, on the strength of the magnetic field.

We now turn to a presentation of the experimental data for the electron-ion oscillations: axially symmetric modes are considered in Sec. 1 and modes that do not exhibit axial symmetry are considered in Sec. 2.

[1)] It is evident that in the one-dimensional case (k_z = k) the relation in (7) is identical with the instability condition (1).

[2)] A spatially uniform beam can also exhibit modes in which $k_\varphi \neq 0$. However, it is not difficult to see from Eq. (7) that an increase in k^2 would lead to a significant increase in the threshold for the instability.

Instability	Frequency range	Spatial structure	Threshold	Reference
Electron-ion	$\omega = \frac{k_z u}{1+(Mk_z^2/mk^2)^{1/3}}$	$k^2 = k_r^2 + k_z^2$	$I_k = \frac{ma^2}{4e}\frac{k^2u^3}{[1+(mk^2/Mk_z^2)^{1/3}]^3}$	[2-6]
Drift-two stream	$\omega_{Hi} < \omega < k_z u$	$k^2 = k_r^2 + k_z^2 + k_\varphi^2$	$I_k \doteq \frac{ma^2}{4e}\frac{k^2u^3}{1+2k_\varphi u/a\omega_{He}k_z}$	[7-10]
Pierce	Aperiodic $\mathrm{Im}\,\omega \lesssim k_z u$	$k^2 = k_r^2 + k_z^2$	$I_k = \frac{ma^2}{4e}k^2u^3$	[11,12,10]
Electron-electron	$\omega \approx \frac{k_z u}{1+(n_1/n_2)^{1/3}}$	$k^2 = k_r^2 + k_z^2$	$I_k = \frac{ma^2}{4e}\frac{k^2u^3}{[1+(n_2/n_1)^{1/3}]^3}$	[5,6,4,1]

1. ELECTRON-ION TWO-STREAM INSTABILITY

The experiments described here were carried out on an apparatus (Fig. 2) which was used earlier to measure the limiting currents in quasi-neutral electron beams.[10] A monoenergetic beam of electrons with energy $W_1 = 50-1000$ eV propagates along the uniform magnetic field along the axis of a cylindrical vacuum chamber with metal walls. The strength of the magnetic field H can be varied from 100 to 8,000 Oe and satisfies the condition in (3); (also, as will be evident below, the condition $\omega_{Hi} < \omega\, k_z u$ is satisfied, this condition appearing in the second row of the table). The beam radius $a = 0.5$ cm and the cylinder radius $R_0 = 15$ cm while the length of the beam L can be varied from 10 to 100 cm ($a \ll R_0$ and usually $R_0 \ll L$). The beam current is varied from milliamperes to hundreds of milliamperes. The ions that neutralize the space charge in the beam are produced by the beam itself by ionization of the background gas in the vacuum chamber. The gas pressure p is approximately 1×10^{-6} mm Hg. Under these conditions the beam exhibits a small negative potential with respect to the wall and the ion density n_+ is essentially equal to the density of electrons in the beam n_1 while the density of plasma electrons can be neglected.

In order to investigate the spatial structure of the waves we use four electrostatic probes in the form of discs; these discs are 0.8 cm in diameter and are located in the central cross-section of the apparatus at various azimuthal angles, separated by 90°; the radial positions are the same for all probes. One of these probes can also be moved freely along the beam. The apparatus is also provided with an analyzer for transverse ion energy which has been described earlier in[13]. The measurement of the plasma ion density and the beam electron density (as well as the radial distribution of these quantities) was carried out by means of a differential anode method proposed by A. V. Zharinov which has been used, in particular, in[14]. The potentials of the anode and the "cathode" grids (Fig. 2) are set equal to zero.

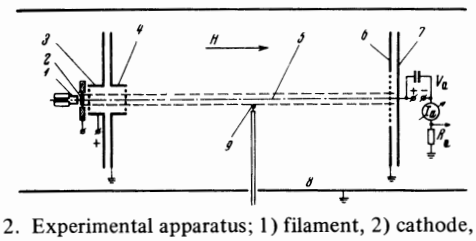

FIG. 2. Experimental apparatus; 1) filament, 2) cathode, 3, 4, 6) diaphragms; 5) beam; 7) anode; 8) vacuum chamber; 9) electrostatic probe.

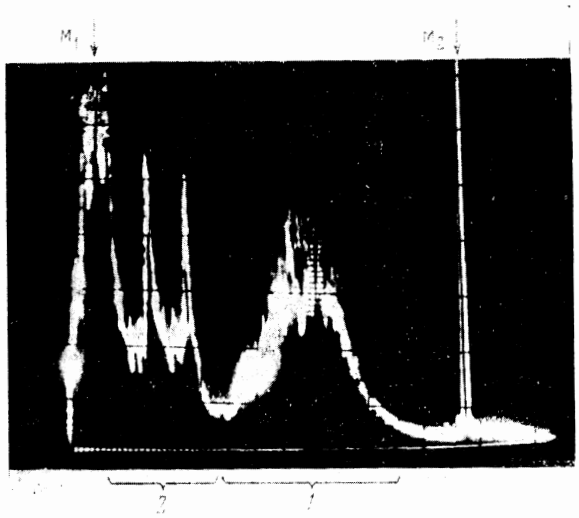

FIG. 3. Frequency spectrum for electron-ion oscillations. 1) Oscillations characterized by axial symmetry; 2) oscillations characterized by a lack of axial symmetry. Frequency markers: $f_{m1} = 0$, $f_{m2} = 1500$ kHz, the energy of the beam electrons $W_1 = 150$ eV, the beam current $I \approx 25$mA, $H = 3500$ Oe, $L = 70$ cm, $p = 2 \times 10^{-6}$ mm Hg and the radial position of the probe is given by $R_{pr} = 4$ cm.

In the system described here (however at appreciably higher gas pressures $p \approx 10^{-5}$ mm Hg, where the plasma electron density n_2 is not small compared with the beam density n_1) there are electron oscillations at frequencies of the order of 3–30 MHz. These oscillations were described in[1] in which it was shown that the threshold for the excitation of the oscillations and the dispersion relations are in good agreement with the theory of the conventional two-stream electron-electron instability, corresponding to the fourth column of the table where $k_z = n\pi/L$, n is an integer (usually between 1 and 10).

In contrast with these oscillations, those found at $p \approx 10^{-6}$ mm Hg (in which case $n_2 \ll n_1$) are relatively low frequency oscillations: $\omega \ll k_z u$; furthermore for this case $n = 1$. These oscillations are characterized by a different kind of axial symmetry. A typical frequency spectrum (taken with an S4-8 analyzer) is shown in Fig. 3. The left portion of this spectrum corresponds to waves that do not exhibit axial symmetry and which are considered in Sec. 2 of the present paper. The right portion of the spectrum in Fig. 3 corresponds to axially symmetric waves. The existence of this symmetry is verified by the coincidence of the phase of signals obtained from the four electrostatic probes described above. This phase coincidence is illustrated in Fig. 4a, in which we show oscillograms of the signals from one pair of diametrically opposed probes. For purposes of comparison, in Fig. 4b we show waves that do not exhibit axial symmetry.

These waves are electron-ion waves. This feature follows from the fact that the excitation of the oscillations is accompanied by the acceleration of ions to comparitively high energies, energies of the order of the electron energy in the beam. This feature follows from the experimental data shown in Fig. 5, which

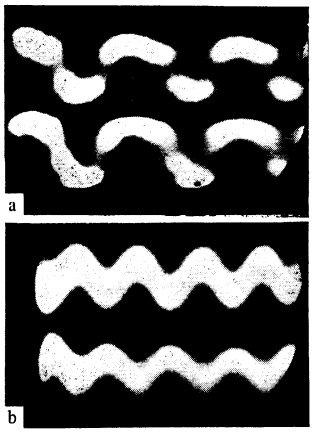

FIG. 4. Oscillograms showing signals from two electrostatic probes located at a relative azimuthal angle of 180°: a) electron-ion oscillations characterized by axial symmetry; oscillation frequency f_c = 700 kHz, W_1 = 140 eV, I = 20 mA, L = 90 cm, H = 3300 Oe, and p = 2 × 10^{-6} mm Hg; b) electron-ion oscillations characterized by a lack of axial symmetry; oscillation frequency f_0 = 240 kHz, W_1 = 105 eV, I = 10 mA, L = 90 cm, H = 1000 Oe and p = 1 × 10^{-5} mm Hg (nitrogen).

gives the dependence of the transverse energy of the nitrogen ions $W_\perp$ and the amplitude of the axially symmetric waves on beam current. A measure of $W_\perp$ in this case is the magnitude of the potential applied to the electrode in the ion energy analyzer. It is evident that appreciable excitation and ion acceleration start at some threshold current ($I = I_k \approx 16$ mA).

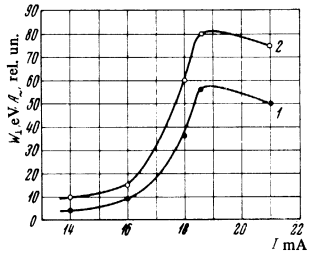

FIG. 5. The ion energy $W_\perp$ (curve 2) and the amplitude of the axially symmetric electron-ion oscillation (1) as functions of the beam current. The ion energy analyzer is located at the radius R_{pr} = 8 cm; H = 2600 Oe, L = 90 cm, p = 1 × 10^{-6} mm Hg, W_1 = 150 eV.

The dispersion properties of the axially symmetric waves are shown in Figs. 6–9. In Fig. 6 we show frequency spectra taken for three different values of the beam current. The waves appear at a critical current, and as the beam current increases the wave frequency is reduced considerably. In Figs. 7 and 8 we show the frequency[3] f_c as a function of electron velocity u and beam length L. It is evident that over the largest part of the range of variation of these parameters there is a relation of the form $f_c \sim u/L$. The oscillation frequency f_c is essentially independent of the strength of the magnetic field (when $L \lesssim 50$ cm) or only a very weak function of the field.

An especially important feature is the fact that the oscillations lead to the formation of standing waves along the beam (Fig. 9a). The wavelength (first harmonic) is found to be equal to twice the beam length: $\lambda_z \approx 2L$, $k_z \approx \pi/L$. Taking account of this feature, from Figs. 7–9a we find

$$\omega_c \equiv 2\pi f_c \approx \left(\frac{1}{4} \div \frac{1}{5}\right) k_z u. \qquad (11)$$

The conditions for excitation of the axially symmetric waves are shown in Figs. 10 and 11 which indicate the dependence of the excitation current I_c on the electron velocity in the beam and the strength of the magnetic field. The limiting values of the beam current I_l can also be obtained from these figures; the reason for the limitation on beam current is discussed in Section 2. The following clearly defined features are of interest:

$$I_c \sim u^3, \quad I_c \neq f(H), \quad I_c \approx 0.5 I_P, \qquad (12)$$

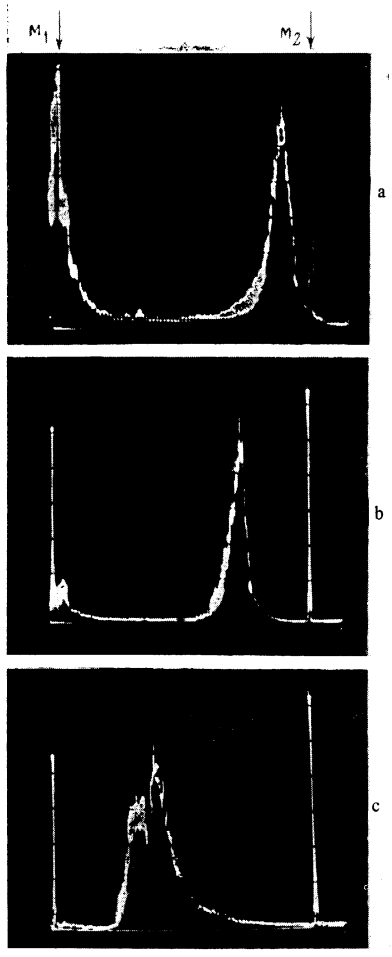

FIG. 6. Frequency spectra for oscillations characterized by axial symmetry. The frequency markers are located at f_{m1} = 0, f_{m2} = 1500 kHz; W_1 = 300 eV, H = 4000 Oe, L = 90 cm, p = 3 × 10^{-6} mm Hg (nitrogen). The probe radius R_{pr} = 6 cm. a) I = 52 mA, b) I = 59 mA, c) I = 64 mA. The oscillation amplitudes for a, b and c are in the ratio 1:2.5:2.5. The critical current I_c = 50 mA.

FIG. 7. The frequency of the axially symmetric electron-ion oscillations f_c as a function of the energy of the beam electrons, $W_1 = mu^2/2$, H = 7800 Oe, L = 90 cm, p = 1.5 × 10^{-6} mm Hg. The oscillation frequency is measured at the the critical beam current $I = I_c$.

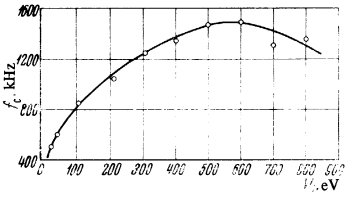

FIG. 8. The frequency of the axially symmetric electron oscillation f_c as a function of beam length. W_1 = 150 eV, H = 7800 Oe, and p = 1 × 10^{-6} mm Hg. The oscillation frequency is measured at the critical beam current $I = I_c$.

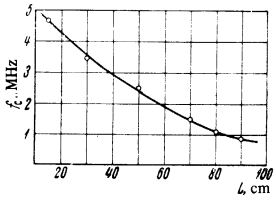

[3] The subscript "c" will be used hereafter to denote the characteristics of the electron-ion waves with axial symmetry.

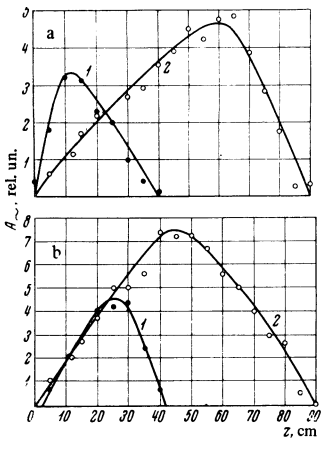

FIG. 9. The amplitude distribution of the electron-ion oscillations over the length of the beam. A_2 is the alternating component of the current to the moveable probe which is located at a distance R_{pr} = 5 cm from the beam axis, the probe diameter is 8 mm and the probe coordinate Z is measured from the beam source. a) Axially symmetric oscillations: 1) L = 45 cm, f_c = 1.6 MHz, W_1 = 150 eV, H = 2600 Oe, I = 18 mA; 2) L = 90 cm, f_c = 0.85 MHz, W_1 = 150 eV, H = 3100 Oe, I = 22 mA. b) Asymmetric oscillations: 1) L = 45 cm, 2) L = 90 cm, f_0 = 300 kHz, W_1 = 150 eV, H = 1300 Oe, I = 12 mA, p = 1.8 × 10^{-6} mm Hg.

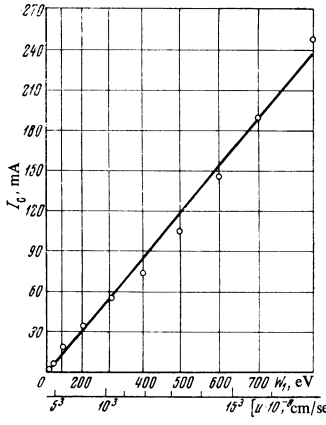

FIG. 10. The critical current for excitation of axially symmetric electron-ion oscillations I_c as a function of the cube of the velocity of the beam electrons. H = 7800 Oe, L = 90 cm, p = 1.4 × 10^{-6} mm Hg.

where I_P is the excitation current for the Pierce instability (the third column in the table).

It will be evident that all of the wave properties that have been described, such as the excitation threshold, the spatial structure, and the dispersion characteristics, are in good agreement with the properties of the electron-ion (Buneman) oscillations, the theory of which has been given above. This can be seen from a comparison of Eqs. (11) and (12) with the theoretical relations in Eqs. (6)—(8) and the first row of the table.

Thus, these waves represent the usual two-stream (electron-ion) instabilities, in the dynamics of which the drift effects associated with the spatial inhomogeneity of the beam does not play an important role. This result is quite natural since it will be shown (Sec. 2) that under the conditions of the experiments described above the current I_c required for excitation of the axially symmetric oscillations is much smaller than the critical current I_k for the excitation of the drift-two-stream electron instability.

2. DRIFT-TWO-STREAM INSTABILITY AND ION ACOUSTIC WAVES IN AN INHOMOGENEOUS PLASMA

1. Dispersion Properties

In the present section we shall discuss the oscillations that correspond to the left portion of the spectrum

FIG. 11. The threshold (critical current) for excitation of various instabilities as a function of magnetic field: 1) I = I_c the threshold for excitation of axially symmetric electron-ion oscillations; 2) I = I_l the limiting beam current; 3) I = I_p the current for excitation of the Pierce instability.[10,11,12] W_1 = 200 eV, L = 90 cm, p = 4 × 10^{-6} mm Hg.

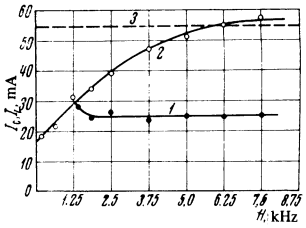

in Fig. 3, these oscillations being characterized by a lack of axial symmetry. The lack of axial asymmetry is established by taking oscillograms of signals from the four electrostatic probes described above: the signals from diametrically opposed probes exhibit opposite phase (Fig. 4b) while the signals from adjacent probes exhibit a phase shift of 90°. The sign of the indicated phase shifts corresponds to propagation of a wave in the direction of Larmor gyration of an electron in the magnetic field. The amplitude of the current oscillations of the probe is comparable with the steady component. These oscillations lead to the formation of standing waves along the beam with wavelength (fundamental) $\lambda_Z = 2\pi/k_Z \approx 2L$ (cf. Fig. 9b).

A frequency spectrum of these waves is shown in Fig. 3 (cf. left side of the figure). It is evident that the spectrum consists of the fundamental f_0 and its second harmonic. In Figs. 12 and 13 we show the dependence of the frequency f_0 on the ion density in the plasma for two nitrogen pressures: p = 2 × 10^{-5} mm Hg and p = 9 × 10^{-5} mm Hg. Under the conditions corresponding to Figs. 12 and 13 the plasma density is controlled by changing the beam current. It is evident that at relatively small plasma densities ($n_+ \lesssim 10^8$ cm^{-3}) the quantity f_0 varies as $\sqrt{n_+}$ to with an accuracy of approximately 25% and corresponds to the ion plasma frequency for nitrogen; at higher densities ($n_+ \gtrsim 10^9$ cm^{-3}) the quantity f_0 no longer depends on n_+ and, to the same accuracy of approximately 25%, corresponds to the ion-acoustic frequency $f_0 \approx kV_S/2\pi$

FIG. 12. The frequency of the electron-ion oscillations as a function of plasma density for a nitrogen pressure p = 2 × 10^{-5} mm Hg, W_1 = 150 eV, H = 1300 Oe, L = 10 cm. The dashed curve shows the plasma frequency for molecular nitrogen ions $f_+ = \omega_+/2\pi = \sqrt{n_+e^2/\pi M}$ divided by the factor 1.2

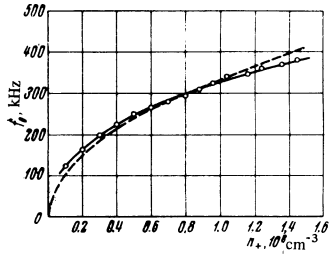

FIG. 13. 1) The frequency of the electron-ion oscillations as a function of plasma density for a nitrogen pressure p = 9 × 10^{-5} mm Hg, W_1 = 150 eV, H = 1300 Oe, L = 10 cm. 2) The frequency of the ion-acoustic wave $f_S = w_S/2\pi = kV_S/2\pi = (k/2\pi)\sqrt{T_e/M}$ multiplied by the factor 1.25; T_e = 10 eV, nitrogen. The small beam length (L = 10 cm) is chosen to reduce the noise due to the flute instability.

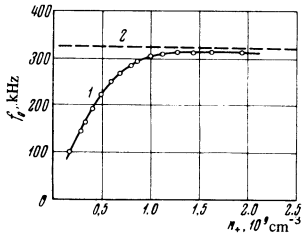

where $V_s = \sqrt{T_e/M}$ is the ion-acoustic velocity, T_e is the temperature of the plasma electrons (we take $T_e \approx 10$ eV, cf. below), M is the ion mass and $k^2 = k_z^2 + k_r^2 + k_\varphi^2 \approx 2/a^2 \approx 8\ cm^{-2}$. A reduction in beam radius a leads to an increase in the frequency f_0, which goes approximately as 1/a (Fig. 14). The frequency is found to be relatively insensitive to other system parameters such as the energy of the primary electrons, the beam length, the magnetic field and the gas pressure.

It will be evident that the frequency of these waves is described with good accuracy by the relation

$$\omega^2 \approx \frac{\omega_+^2}{1 + 1/k^2d^2} \qquad (13)$$

where $d = \sqrt{T_e/4\pi n_2 e^2}$ is the electron Debye radius, T_e and n_2 are the temperature and density of the plasma electrons. Under the conditions corresponding to Fig. 12, for example with $n_+ \approx 0.5 \times 10^8\ cm^{-3}$, $T_e = 10$ eV, $k_z = \pi/L$, $k^2 \approx 8\ cm^{-2}$ and $1/k^2d^2 \approx 0.34$, we find, in accordance with Eq. (13), that $\omega \approx \omega_+$. On the other hand, for the conditions corresponding to Fig. 13, for example with $n_+ \approx 10^9\ cm^{-3}$, $1/k^2d^2 \approx 7 \gg 1$, Eq. (13) yields $\omega \approx kV_s$, which corresponds to the experimental data shown in Figs. 12 and 13.

When the beam radius is reduced by a factor of 2 the quantity k^2 is increased by approximately a factor of 4. Consequently, the function $f_0(n_+)$ should reach saturation at a value of d^2 that is four times smaller than for the previous beam radius. For this to occur it is necessary that the current corresponding to saturation for the dependence $f_0(n_+)$ remain the same. However, it is found that when the beam radius is reduced by a factor of two the current exceeds the limiting current of the beam (cf. below). Hence, there is no doubt that for a cathode radius of 0.25 cm the function $f_0(n_+)$ does not reach saturation (Fig. 14).

A control experiment for verifying the dispersion relation in Eq. (13) could be carried out by measuring the dependence of oscillation frequency on ion mass. We have not carried out this experiment because it has actually been done in work reported by a number of authors[15-17] under conditions approximately the same as those reported here; these authors have also observed ion oscillations in electron beams. The results of the measurements made in these experiments with different ion masses (helium, nitrogen and other gases) can be combined to exhibit the general feature: $\omega \approx \omega_+$. Under the conditions pertaining to this work the quantity $1/k^2d^2$ was much smaller than unity so that the ion density was not an important feature in the excitation of the ion-acoustic branch.

2. Effects Due to Oscillations

The excitation of these oscillations is undoubtedly accompanied by accleration of plasma ions to appreciable energies and by the anomalous diffusion of plasma particles across the strong magnetic field. The first of these effects is shown in Fig. 15, in which we indicate the dependence of ion energy $W_\perp$ and oscillation amplitude on nitrogen pressure. It is evident that the ion energy is approximately equal to the energy of the beam electrons. At the same time the amplitude of the oscillations of the plasma potential, as indicated by

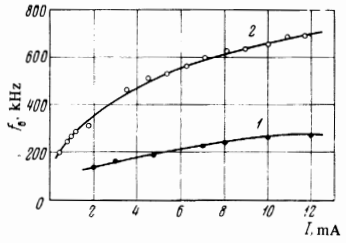

FIG. 14. The frequency of the electron-ion oscillations as a function of beam current for two-beam diameters: 1) 2a = 1 cm, 2) 2a = 0.5 cm, W_1 = 150 eV, H = 1300 Oe, $p = 5 \times 10^{-5}$ mm Hg, L = 10 cm.

probe measurements, is approximately 10 V, that is to say, approximately one order of magnitude smaller than $W_\perp/e$. This means that the acceleration of ions by the electric fields in the waves occurs as a multiple-step process as is the case, for example, in cyclical particle accelerators. However, this acceleration is not a resonance process: the frequency of the waves is appreciably greater than the ion gyrofrequency. The observations indicate that these waves (like the drift waves in a thermal plasma[18]) experience a random modulation of amplitude and phase. The mean time for this modulation process τ is a strong function of the system parameters and for a sufficiently high beam current is found to be of the order of 10 oscillation periods. Hence, the multiple-step acceleration of the ions occurs in random fashion[19,20] and it can be pictured as the result of random impulses (with mean lifetime τ) on a harmonic oscillator.[21] The density of accelerated ions was not measured in these experiments. In other experiments described in[13] the density of ions accelerated to energies $W_\perp \approx W_1$ did not differ very much from the total plasma density.

The second effect that accompanies the electron-ion oscillations is the significant increase in the characteristic transverse dimension (radius) of the plasma. The radius of the primary beam is also increased, although to a lesser degree (this is reasonable since the primary electrons are subject to the effect of the wave fields for an appreciably shorter time). This feature is shown in Fig. 16, where we indicate typical radial distributions of ion density and electron density in the beam. It will be evident that when $p \approx (1-3) \times 10^{-6}$ mm Hg the plasma radius R is appreciably greater than the radius of the primary electron beam a: $R^2/a^2 \approx 6$. This relation between R^2 and a^2 is maintained up to gas pressures $p \approx 5 \times 10^{-5}$ mm Hg

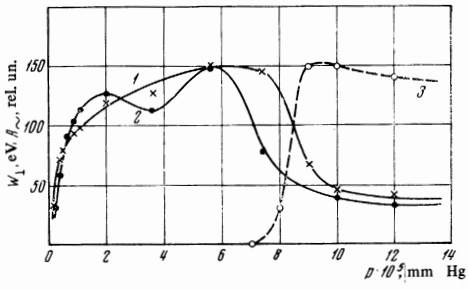

FIG. 15. The amplitude of the low-frequency current oscillations at the probe (2) and the energy of the accelerated nitrogen ions (1) as functions of nitrogen pressure. W_1 = 150 eV H = 1300 Oe, L = 90 cm and I = 15 mA. The waves propagate around the beam axis in the electron direction and the oscillation frequency is of the order of 300 kHz. The curve marked 3 is the amplitude of the wave at frequency f = 50 kHz that propagates in the ion direction.

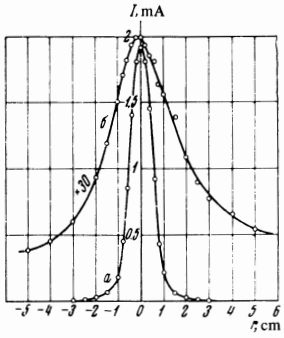

FIG. 16. The radial distribution of the ion density (b) and the distribution of the primary electrons (a). Along the ordinate axis is plotted the values of the ion current and the electron current in the beam to the collector of the differential anode which has the following potentials 400 and OV, W_1 = 150 eV, H = 1300 Oe, L = 90 cm, p = 5 × 10^{-5} mm Hg. It is evident that $R^2/a^2 \approx 6$, a ≈ 0.7 cm.

(for a beam length L ≈ 100 cm). When p ≈ 1 × 10^{-4} mm Hg the radii R and a are found to be approximately the same: $R^2 = a^2$. The reduction in the ratio R^2/a^2 at high gas pressure is due to the corresponding reduction in wave amplitude (Fig. 15).

3. Excitation Mechanism at Small Beam Currents

The excitation of these waves occurs at relatively small beam currents, much smaller than the limiting current (cf. Figs. 12 and 13). According to the theories[22,7] and instability of this kind [axially asymmetric oscillations (13)] can occur in the absence of a beam by what is essentially the same mechanism as that responsible for the drift ("universal") plasma instability. It is necessary that the plasma exhibit a sufficiently strong inhomogeneity in space, that is to say, the following condition must be satisfied:

$$kV_s > \omega_{Hi} \text{ or } \rho_{Li} > a, \qquad (14)$$

where $\rho_{Li} = \sqrt{MT_e}\,c/eH$ is the ion Larmor radius corresponding to the electron temperature. Furthermore, it is necessary that the plasma be nonisothermal: the electron temperature T_e must be considerably greater than the ion temperature T_+ because if this is not the case the waves will be subject to strong ion-Landau damping. We note at the outset that in the present experiments, in which the gas pressure is not too high, the condition $T_e \gg T_+$ is satisfied since the electrons formed in the gas by the beam obtain an energy of the order of the ionization potential of the gas atoms; the ions acquire a much smaller energy. The inequality in (14) for nitrogen atoms with T_e = 10–15 eV also corresponds to the present experimental conditions. The waves that are excited should propagate in the direction of electron gyration.

The mechanism discussed here is called a kinetic mechanism since it is associated with resonance electrons that propagate along the magnetic field with velocities close to the longitudinal phase velocity of the wave ω/k_z. It is not difficult to see that this mechanism corresponds to the properties described above for the axially asymmetric electron-ion waves observed at small beam currents. If this point of view is adopted it is also easy to explain the result (Fig. 15) that the wave amplitude reaches a peak at a nitrogen pressure p ≈ (3–5) × 10^{-5} mm Hg and is reduced with further increase in this pressure (that is to say, as the plasma density is increased). The point here is, as follows from Fig. 15, that simultaneously with the reduction in amplitude of the waves there arise other waves at frequencies of approximately 50 kHz. These latter waves have a different spatial structure: they correspond to the rotation of a flute around the axis of the beam in the "ion" direction and, as indicated in,[23] can be attributed to the centrifugal flute instability characteristic of a plasma. The appearance of these waves is accompanied by a reduction in electron temperature T_e: the latter varies from $T_e \approx 10$ eV at p ≈ 5 × 10^{-5} mm Hg to $T_e \approx 2$–3 eV at p ≈ 1 × 10^{-4} mm Hg. The last result means that the condition in (14) no longer holds and the wave amplitude is reduced.

It should be noted, as has already been indicated in in,[23] that an important role in the excitation of these waves is played by electrons produced by secondary omission, these electrons being produced at the collector by the beam electrons. The oscillations described by the dispersion relations in (13) for $k^2d^2 \ll 1$ might be called high-frequency ion-acoustic waves ($\omega \approx kV_s \gg k_zV_s$) in contrast with the low frequency ion-acoustic waves ($\omega \approx k_zV_s$) that are important when the inverse relation to (14) is satisfied.

4. Excitation Mechanism at High Beam Currents

In subsection 3 we have considered a possible mechanism for the excitation of axially asymmetric electron-ion waves (13) at low beam currents. However, our experimental data indicate that at large beam currents (close to the limiting value) a new and more intense mechanism for the excitation of oscillations comes into play. This feature is evident from Fig. 17, in which we show the oscillation amplitude as a function of beam current. It is evident that at some critical current I_k there is a new and sharply defined growth

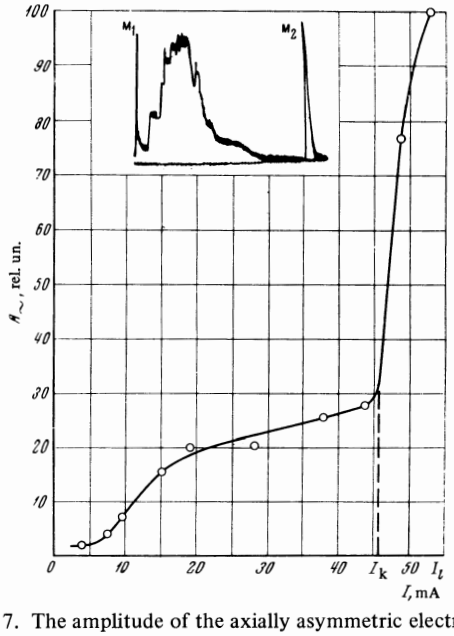

FIG. 17. The amplitude of the axially asymmetric electron oscillations as a function of beam current. W_1 = 300 eV, H = 2000 Oe, L = 100 cm and p = 2 × 10^{-6} mm Hg. In the insert we show the frequency spectrum of the oscillations directly before the cutoff of the beam current, I = 48 mA; the sharp peaks are frequency markers: $f_{m1} = 0$ and f_{m2} = 1200 kHz.

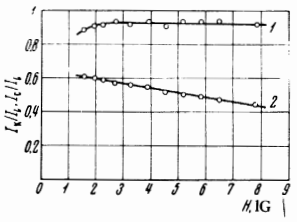

FIG. 18. The dependence of the ratios I_k/I_l (1) and I_c/I_l (2) on magnetic field. W_1 = 150 eV, L = 90 cm, p = 0.7 × 10^{-6} mm Hg.

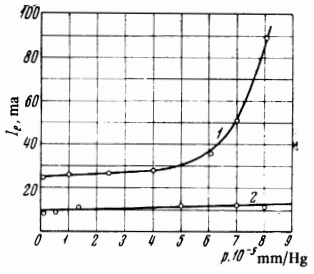

FIG. 19. The limiting current in the electron beam as a function of gas pressure. W_1 = 150 eV, H = 1300 Oe, L = 10 cm. 1) beam diameter 1 cm, 2) beam diameter 0.5 cm. When p = 8 × 10^{-5} mm Hg (case 1) $n_2/n_1 \approx 5-6$. At higher pressures ($n_2/n_1 > 5-6$) the limitation (cutoff) of the beam current does not occur.

in the wave amplitude and when $I = I_l$ there is a discontinuity in the beam current (under these conditions a virtual cathode is formed in the beam[10]). The limiting beam current I_l exceeds the current I_k by approximately 10–15%, as follows from Figs. 17 and 18.

We have indicated above that the experiments described in this section were carried out with the purpose of verifying the theory of the drift-two-stream instability. For this reason it is most desirable to compare the experimentally observed threshold current I_k (which, in accordance with Figs. 17 and 18 we will identify with the limiting beam current I_l) with the theoretical current for the excitation of the drift-two-stream instability as determined by Eq. (9) and the second column in the table. In order to carry out this comparison we consider the following experimental data.

1. We first consider Fig. 11 which shows the dependence of the current I_k on magnetic field. It will be evident that when H increases the current I_k first increases rapidly and then essentially reaches a maximum. For relatively small values of H ($H \lesssim 1250$ Oe) the current I_k is smaller than the current I_c for the excitation of electron-ion waves which exhibit axial symmetry and for larger values of H the current I_k exceeds I_c by a factor of 2.5. It will be evident that the nature of the function $I_k(H)$ and the indicated sequence of excitation (axially symmetric and axially asymmetric waves) as a function of magnetic field are in good agreement with the theoretical relations (7)–(9) and the first two rows of the table.

2. It has been shown in detail in[10] that the limiting beam current I_l (i.e., in accordance with Figs. 17 and 18 the current I_k) is in good agreement with the relation (9) under the following assumptions with respect to the spatial structure of the waves:

a) the waves do not exhibit axial symmetry and are characterized by $k_\varphi \equiv s/a \approx 1/a$;

b) $k_z = \pi/L$ (more precisely, in[10] the value of k_z was double the actual value and the value of a^2 was one half: 0.25 cm^2 in place of the observed value of 0.5 cm^2 (Fig. 16), but the product $k_z a^2$ that appears in (9) remains the same).

These assumptions correspond to the experimental data given in subsection 1 of the present section (cf. for example, Fig. 9b and the spectrum analyzer result in Fig. 17). It was also shown in[10] that the experimentally observed relation between the limiting current I_l and the Pierce current Ip corresponds to the data given in the table.

3. The verification of Eq. (9) in[10] was carried out by changing the electron energy in the beam $W_1 = mu^2/2$ and the strength of the magnetic field. An additional way of verifying Eq. (9) is to change the beam radius a. It is evident from Eq. (9) that since $k^2 \sim 1/a^2$ the quantity I_k can depend on a only if the second "drift" term in the denominator in (9) is not small compared with unity. A comparison of the limiting currents I_l for different beam radii is given in Fig. 19. It is evident that a reduction in cathode radius from 0.5 to 0.25 cm (with W_1 = 150 eV, H = 1300 Oe, L = 10 cm) leads to a reduction of I_l by approximately a factor of 2.5 whereas with s = 0 the reduction factor should not be bigger than 1.16.

4. According to the theory,[7] if a quasi-neutral electron beam produces "surplus" plasma the critical current for excitation of the drift two-stream instability is increased. In order for the drift two-stream instability to be excited the density of surplus plasma n_z cannot exceed the value given by the relation

$$n_2 / n_1 \approx R^2 / a^2, \qquad (15)$$

where R is the "radius" of the plasma. In order to verify Eq. (15) we have examined the dependence of the limiting beam current on plasma density as controlled by varying gas pressure. This dependence is shown in Fig. 19. It is evident that when the plasma density $n_2 \approx n_+$ reaches a value (5–6) n_1 and $R^2 \approx (4-5)\,a^2$, that is to say, when the relation in (15) is satisfied approximately, the discontinuity in beam current (an indicator of the instability) is no longer observed. In this connection we should note that the absence of a sharp dependence of I_l (n_+) on the small radius of the beam (Fig. 18) also corresponds to the criterion in (15).

Finally, we note that when $I > I_k$ there is (a more intense) excitation of the axially asymmetric electron-ion waves which exist when $I < I_k$; this is also to be expected because these waves have the "required" spatial structure and lie in the "required" frequency range (see the second row of the table).

The experimental facts indicate that the excitation of axially asymmetric electron-ion waves observed under the present experimental conditions when $I \geq T_k$ is a direct consequence of the electron-ion drift-two-stream instability with threshold given by (9). This instability is accompanied by two well-defined effects-the limitation (cutoff) in the current of the electron beam in the plasma and the acceleration of plasma ions to relatively high energies: $W_\perp \approx W_1$. (The effect of this instability on the propagation of an electron beam in a dense plasma ($n_2 \gg n_1$) is treated in[23].) As shown in[13] the instability of an electron beam in a plasma discussed here can be exploited to fill magnetic traps to ion densities $n_+ \approx 10^{11}$ cm^{-3} with mean energies $W_\perp \approx 1$ keV.

CONCLUSION

The experimental data presented above indicate that electron-ion instabilities with excitation thresholds given in the table are actually observed in these experiments. These instabilities appear in the excitation of waves whose spatial structure and basic dispersion properties are in agreement with the theoretical predictions. The results obtained in these experiments also provide a verification for the existing linear theory of two-stream instabilities.

In conclusion we wish to make an interesting comparison. Let us compare the condition in (10), for which the drift two-stream instability is very different from the usual two-stream instability, with the condition for the drift ("universal") instability of a Maxwellian plasma. As is well known[22,7] the latter condition is given by

$$v_z k_\varphi / a\omega_{He} k_z > 1, \qquad (16)$$

where $v_{Ti} < v_z < v_{Te}$ and $v_z = \omega/k_z$ is the velocity of the resonance electrons which excite the drift wave with frequency ω and the quantities v_{Ti} and v_{Te} are the thermal velocities of the ions and electrons in the plasma. It will be evident that the conditions in (10) and (16) are physically equivalent. This feature illustrates the fact[7] that the origin of the drift-two-stream instability ([given by the condition in (10)] is the same physical mechanism that is responsible for the drift instability in a Maxwellian plasma. The experimental investigation of this mechanism is found to be most convenient for the case of a delta-function distribution of electron velocities (beam) as a consequence of the existence of a threshold (9); in the case of a Maxwellian electron velocity distribution, it is evident from (16) that there is no analogous threshold.

Thus, the simple beam experiments carried out in the present work make it possible to model the mechanism for a plasma instability which is of great interest from the point of view of confinement of a stable high-temperature plasma.

[1] M. V. Nezlin, G. I. Sapozhnikov and A. M. Solntsev, Zh. Eksp. Teor. Fiz. 50, 349 (1966) [Sov. Phys. JETP 23, 232 (1966)].

[2] G. I. Budker, Atomnaya énergiya (Atomic Energy) 5, 9 (1956).

[3] O. Buneman, Phys. Rev. 115, 503 (1959).

[4] A. A. Vedenov, E. P. Velikhov and R. Z. Sagdeev, Usp. Fiz. Nauk 73, 701 (1961) [Sov. Phys.-Usp 4, 332 (1961)].

[5] M. F. Gorbatenko and V. D. Shapiro, Coll. Vzaimodeĭstvie puchkov zaryazhennykh chastits s plazmoĭ (Interaction of Charged-particle Beams with a Plasma) Naukova dumka, Kiev, 1965, p. 103.

[6] Ya. B. Faĭnberg, Atomnaya énergiya (Atomic Energy) 11, 313 (1961).

[7] A. B. Mikhaĭlovskiĭ, Zh. Tekh. Fiz. 35, 1945 (1965) [Sov. Phys.-Tech. Phys. 10, 1498 (1966)]; Atomnaya énergiya (Atomic Energy) 20, 103 (1966).

[8] L. S. Bogdankevich, E. A. Lovetskiĭ and A. A. Rukhadze, Nuclear Fusion 6, 176 (1966).

[9] V. V. Vladirmirov, Dokl. Akad. Nauk SSSR 162, 785 (1965) [Sov. Phys. Dokl. 10, 519 (1965)].

[10] M. V. Nezlin and A. M. Solntsev, Zh. Eksp. Teor. Fiz. 53, 437 (1967) [Sov. Phys. JETP 26, 290 (1968)].

[11] J. R. Pierce, J. Appl. Phys. 15, 721 (1944).

[12] J. Frey and C. K. Birdsall, J. Appl. Phys. 37, 2051 (1966).

[13] M. V. Nezlin and A. M. Solntsev, Zh. Eksp. Teor. Fiz. 45, 840 (1963) [Sov. Phys. JETP 18, 576 (1964)].

[14] M. V. Nezlin and A. M. Solntsev, Zh. Eksp. Teor. Fiz. 49, 1377 (1965) [Sov. Phys. JETP 22, 949 (1966)]

[15] V. D. Fedorchenko, B. N. Rutkevich, V. I. Muratov and B. M. Chernyi, Zh. Tekh. Fiz. 32, 958 (1962) [Sov. Phys.-Tech. Phys. 7, 696 (1963)].

[16] K. G. Hernquist, J. Appl. Phys. 26, 544 (1955).

[17] A. Vermeer, T. Matitti, H. J. Hopman and J. Kistemaker, Plasma Physics 9, 241 (1967).

[18] N. S. Buchel'nikova, R. A. Salimov and Yu. I. Éĭdel'man, Zh. Eksp. Teor. Fiz. 52, 837 (1967) [Sov. Phys. JETP 25, 548 (1967)].

[19] E. L. Bershteĭn, V. I. Veksler and A. A. Kolomenskiĭ, Nekotorye voprosy teoriĭ tsiklicheskikh uskoriteleĭ (Certain Problems in the Theory of Cyclic Accelerators) Acad. Sci. USSR Press, 1965, p. 3.

[20] A. A. Kolomenskiĭ and A. N. Lebedev, Teoriya tsiklicheskikh uskoriteleĭ (Theory of Cyclic Accelerators), Fizmatgiz, 1962, p. 322.

[21] G. S. Gorelik, Kolebaniya i volny (Oscillations and Waves) Fizmatgiz, 1959.

[22] B. B. Kadomtsev, Plasma Turbulence, Academic Press, 1964.

[23] M. V. Nezlin, Zh. Eksp. Teor. Fiz. 53, 1180 (1967) [Sov. Phys. JETP 26, 693 (1968)].

Translated by H. Lashinsky
47